Quantum Transport of Massless Dirac Fermions

Kentaro Nomura and A. H. MacDonald

Department of Physics, University of Texas at Austin, Austin Texas 78712-1081, USA

(Received 22 June 2006; published 14 February 2007)

Motivated by recent graphene transport experiments, we undertake a numerical study of the conductivity of disordered two-dimensional massless Dirac fermions. Our results reveal distinct differences between the cases of short-range and Coulomb randomly distributed scatterers. We speculate that this behavior is related to the Boltzmann transport theory prediction of dirty-limit behavior for Coulomb scatterers.

DOI: 10.1103/PhysRevLett.98.076602 PACS numbers: 72.10.−d, 73.21.−b, 73.43.−f, 73.50.Fq

Introduction.—Graphene can be described at low energies by a four component massless Dirac-fermion (MDF) model [1] that has long attracted theoretical attention because of appealing properties including chiral anomalies [2–5], randomness induced quantum criticality [6–8], relevance to high T_c superconductors [9,10], and various unusual transport properties [5–19]. The recent experimental realization of single-layer graphene sheets [20] has made it possible to confirm a number of theoretical predictions, including unusual quantum Hall effects [21,22], and has also revealed some surprises. The main findings can be summarized as follows: (i) graphene's conductivity σ never falls below a minimum value ($\sigma^{\min}$) corresponding (approximately) to a conductance quantum (e^2/h) per channel, in spite of predictions [6,7,10,13,15] based on the self-consistent Born approximation (SCBA) that $\sigma^{\min} = (1/\pi)e^2/h$ for a MDF channel, and predictions that localization occurs [14,16,17] when intervalley scattering is significant; (ii) in gate-doped graphene σ increases linearly with the carrier density n away from the charge neutrality (Dirac) point, implying a constant mobility $\mu = \sigma/ne$ [21,22] and not the constant conductivity usually predicted for the Boltzmann transport regime [13]. Although these surprises have inspired a number of theoretical studies [15–17], the source of the discrepancies between experiment and theory has not yet been conclusively identified.

We have recently pointed out that the linear dependence of conductivity on carrier density in graphene can be explained in the framework of Boltzmann transport theory by assuming Coulomb scatterers [23] rather than the short-range scatterers assumed, mainly as a practical simplification, in most theoretical work. The golden-rule scattering rate for Coulomb scatterers in a MDF model diverges in the zero energy (Dirac point) limit, whereas it vanishes for short-range scatterers. This property suggests the possibility of a qualitative difference between these two disorder models. Since Boltzmann theory is not applicable in the vicinity of the Dirac point, however, a fully quantum mechanical approach is required to address the minimal conductivity. In this Letter we report on a finite-size Kubo formula analysis used to study the quantum transport of MDFs. Over the range of system sizes that we can describe, we find that $\sigma^{\min}$ is a few times larger for Coulomb scatterers than for short-range scatterers and $\sim e^2/h$.

A two-component MDF model describes graphene transport only when intervalley scattering is unimportant. We argue that the MDF model likely does apply at accessible experimental temperatures to graphene systems near the Dirac point, since the intervalley scattering length obtained within the Born approximation diverges in that limit. The temperature below which intervalley scattering is important should increase away from the Dirac point [24].

Massless Dirac-fermion model.—Graphene's honeycomb lattice has two atoms per unit cell on sites labeled A and B. The low-energy band structure consists of Dirac cones located at the two inequivalent Brillouin zone corners K and K':

$$H_K = \hbar v \boldsymbol{\sigma} \cdot \mathbf{k} = v\hbar \begin{pmatrix} 0 & k_x - ik_y \\ k_x + ik_y & 0 \end{pmatrix}, \quad (1)$$

and $H_{K'} = \hbar v \boldsymbol{\sigma}^t \cdot \mathbf{k}$, where v is the graphene Fermi velocity and the Pauli matrices $\boldsymbol{\sigma}$ act on the sublattice degrees of freedom. For each wave vector $\mathbf{k}$, Eq. (1) has two eigenstates $|\mathbf{k}, \pm\rangle = (|\mathbf{k}, A\rangle \pm e^{i\phi}|\mathbf{k}, B\rangle)/\sqrt{2}$, where $\phi \equiv \tan^{-1}(k_y/k_x)$, and eigenenergies $E_{\mathbf{k},\pm} = \pm\hbar v|\mathbf{k}|$. When intervalley scattering is neglected, the K and K' valleys contribute independently to the conductivity.

Boltzmann theory for doped graphene.—We start by briefly reviewing Boltzmann transport theory applied to graphene since this consideration motivates Coloumb scatterer models. The Boltzmann conductivity $\sigma_0 = (e^2/h) \times (2E_F\tau_0/\hbar) = (e^2/h)2k_F\ell$ is proportional to the transport relaxation time τ_0. For short-range scatterers the Born approximation gives $\hbar/\tau_0 = 2\pi\bar{V}^2\rho_F = (n_i u^2/\hbar v^2)|E_F|$ [13], where $V(\mathbf{r}) = u\sum_I^{N_i} \delta(\mathbf{r} - \mathbf{R}_I)$ is the disorder potential, n_i is the density of scatterers, and ρ_F the density of states at the Fermi level. When the range of the impurity potential is much longer than the lattice spacing of graphene, intervalley scattering is weak [13,14,16].

Note that σ_0 is independent of the carrier density n. Experiment, on the other hand, finds that the mobility $\mu = \sigma/ne$ in graphene is nearly constant except at very low

densities. One plausible explanation for this behavior is that Dirac-fermion scattering is dominated by Coulomb scattering from ionized impurities near the graphene plane, $V(\mathbf{r}) = \sum_I^{N_i} e^2/\epsilon|\mathbf{r} - \mathbf{R}_I|$. Using Fermi's golden rule and approximating the screened Coulomb interaction by [23] $U_{sc}(\mathbf{q}) = (2\pi e^2)/\epsilon(q + 4\alpha_g k_F) \simeq (\hbar v \pi)/(2k_F)$, the Boltzmann conductivity for Coulomb interactions is $\sigma_c \simeq (4e^2/h)(n/n_i)32/\pi$, proportional to density in agreement with experiment. Here $\alpha_g = e^2/\epsilon\hbar v$ is the effective fine structure constant used to characterize the ratio of Coulomb interaction and band energy scales in graphene. ($\alpha_g \simeq 3$ in vacuum and $\simeq 1$ when the graphene sheet is placed on a SiO_2 dielectric substrate.) Note that the Boltzmann conductivity for Coulomb scatterers vanishes as $n \to 0$, contradicting experiment [21].

MDF model finite-size Kubo formula.—Our numerical results, obtained by evaluating the finite-size Kubo formula

$$\sigma = -\frac{i\hbar e^2}{L^2}\sum_{n,n'}\frac{f(E_n) - f(E_{n'})}{E_n - E_{n'}}\frac{\langle n|v_x|n'\rangle\langle n'|v_x|n\rangle}{E_n - E_{n'} + i\eta}, \quad (2)$$

are summarized in Fig. 1. Here $\mathbf{v} = v\boldsymbol{\sigma}$ is the Dirac-fermion velocity operator, $f(E)$ is the Fermi-Dirac function, and $|n\rangle$ denotes an eigenstate of the Dirac equation,

$$[-i\hbar v\boldsymbol{\sigma}\cdot\nabla + V(\mathbf{r})]\psi = E\psi, \quad (3)$$

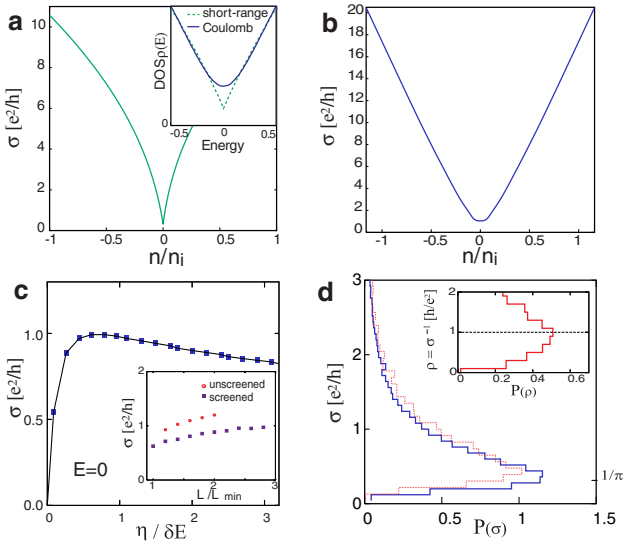

FIG. 1 (color online). Dirac-fermion conductivities for (a) short-range scatterers and (b) screened Coulomb scatterers. The inset of (a) compares the densities of states for short-range and Coulomb cases. (c) Kubo formula conductivities at the Dirac point as a function of η for Coulomb scatterers case. The inset of (c) shows the size dependence of the conductivity for unscreened Coulomb (open circles) and screened Coulomb (boxes) cases. (d) Distribution function of the conductivity and resistivity (inset) at the Dirac point for Coulomb scatterers. In the main panel, the solid (blue) line is for $L = 1.4L_{min}$ and the dotted (red) line is for $L = 2L_{min}$, where L_{min} is the minimum system size considered.

which we solve using a large momentum-space cutoff Λ. The disorder potential momentum-space matrix elements are $\langle \mathbf{k}\sigma|V|\mathbf{k}'\sigma'\rangle = \frac{1}{L^2}\sum_{I=1}^{N_i} U(\mathbf{k} - \mathbf{k}')\delta_{\sigma\sigma'}e^{i(\mathbf{k}-\mathbf{k}')\cdot\mathbf{R}_I}$, where $U(\mathbf{q})$ is constant for delta impurities and given by $U_{sc}(\mathbf{q})$ for the screened Coulomb scattering case. The scattering center locations $\mathbf{R}_I$ and potential signs were chosen at random. We estimate the bulk conductivity by evaluating Eq. (2) at a large number of η values. The Kubo conductivity σ vanishes for both small and large η, but there is an intermediate region where the dependence of σ on η is relatively weak. We use the maximum of σ vs η to estimate the conductivity at a given system size L. For metals, including doped graphene, physical arguments suggest that $\eta \sim \hbar/T_L$, where T_L is the escape time from the system studied numerically. It follows [25] that $\eta \sim \langle\Delta E\rangle \sim g_T\delta E$, where the Thouless energy $\langle\Delta E\rangle$ is the geometric mean of the eigenvalue difference between periodic and antiperiodic boundary conditions, $\delta E = 1/L^2\rho_F$ is the level spacing at the Fermi level, and $g_T \equiv \langle\Delta E\rangle/\delta E$ is the Thouless number.

The reliability of the finite-size Kubo formula method described above is solidly established for diffusive metallic systems [25]. For conventional nonrelativistic two-dimensional electron systems with parabolic dispersion, numerical conductivities calculated in this way agree closely with the theoretical expectation of a Drude conductivity $\sigma_0 = (e^2/h)k_F\ell$ with a finite-size weak-localization correction [26]. Subtleties, related to the η dependence of the numerical estimate, do however arise when this method is applied to insulators. The Dirac point of the MDF model is an intermediate case and related uncertainties apply to our numerical estimate of σ^{min}. The property that the Dirac point density of states is finite in the presence of disorder, as illustrated in the inset of Fig. 1(a), may help validate the Kubo approach. We find that the dependence of σ on η at the Dirac point, illustrated in Fig. 1(c) is similar to that in a metal [25], indicating delocalized states. σ is a maximum when η corresponds to $\sim\delta E$ at each system size as expected for $\sigma \sim e^2/h$. We have also evaluated the Thouless conductivity as a consistency check. A large number of numerical studies have demonstrated that the Thouless conductivity estimate, although perhaps not as accurate in the diffusive metal limit ($\sigma \gg e^2/h$), is more universally applicable. It may be used for both delocalized and strongly localized states [27], and should therefore be reliable at the Dirac point.

Figure 1 compares Kubo conductivity estimates for (a) the short-range scatterer and (b) the screened Coulomb scatterer cases. For the short-range disorder potential case, the density dependence of the conductivity is nonlinear, approaching the constant Boltzmann conductivity for $|E_F| \gg \hbar/\tau$. The estimated value of $\sigma(E = 0)$ is close to the SCBA value $(1/\pi)e^2/h$ predicted in earlier theoretical studies [6,7,10,13,15]. For the screened Coulomb scatterer case, on the other hand, the conductivity σ increases linearly with increasing density $|n|$ as

Boltzmann theory predicts. At the Dirac point, however, the conductivity remains finite with the minimum value $\simeq e^2/h$, which is few times larger than the SCBA value for the short-range model. To illustrate the dependence on carrier density, we have smoothed the curves in Figs. 1(a) and 1(b) by averaging over the Fermi energy interval containing typically 1–30 levels, and over boundary conditions, in addition to over approximately 10^4 disorder realizations.

If we neglect intervalley scattering and account for graphene's spin and valley degeneracies, MDF properties can be compared with graphene experimental results. Both the linear dependence of the conductivity on density and the shift of $\sigma^{\min}$ suggest that long-range scattering similar to that produced by ionized impurities is present in experimental samples. We note that ionized impurities in the substrate or at sample edges that are separated from the conduction channel by a distance that is large compared to the graphene lattice constant but small compared to the Fermi wavelength in the regime studied experimentally ($|n| \lesssim 7 \times 10^{12}$ [cm^{-2}] [21,22]) will act like Coulomb scatterers in the MDF model but will not produce strong intervalley scattering.

The difference between Coulomb and short-range $\sigma^{\min}$ values can be rationalized by the following argument. In the short-range case, the golden rule relaxation time for delta-function scatterers diverges ($\tau_0 \propto 1/|E_F| \to \infty$) at the Dirac point and $k_F\ell$ remains finite. In contrast, Boltzmann transport theory suggests that the Dirac point of the Coulomb scatterer model is in the strong disorder limit because $\tau_c \propto |E_F| \to 0$. We examined this idea by varying the carrier-density n and the ionized impurity density n_i independently, finding that the conductivity for Coulomb scattering model appears to be a function of n/n_i only. Letting $n \to 0$ at finite n_i and letting $n_i \to \infty$ at finite n are equivalent because $\sigma \to \sigma^{\min}$. This finding is consistent with the idea that at the Dirac point MDF Coulomb scatterers are always in the strongly disordered limit. As long as these states remain delocalized, however, the conductivity cannot vanish; the nonzero conductivity at the Dirac point is purely due to the quantum mechanical nature of delocalized states. Although this argument is not quantitative, it makes it clear that there is an essential difference between the Coulomb and short-range cases. A related difference is also seen in the inset in Fig. 1(a) which compares densities of states near the Dirac point ($E = 0$) for short-range scatterers (green dashed line) and Coulomb scatterers (blue solid line). The prominent dip at $E = 0$ in the short-range case is replaced by a smooth minimum at a larger value in the Coulomb case. One interpretation of the increase in Dirac point density of states is that the carrier-density fluctuates spatially in the smooth Coulomb potential. Nonzero local carrier densities at the Dirac point could explain both the increase in density of states and the increase in conductivity. For short-range scatterers, our simulations have focused on the Boltzmann dominated $k_F\ell \gg 1$ regime. We note that systems with $k_F\ell \sim 1$ or smaller behave more like Coulomb scatterer systems at low densities, and have larger minimum conductivities and densities of states.

Although our theory does not account for electron-electron interactions, the issue of screening effect near the Dirac point requires comment. We use the $T = 0$ Thomas-Fermi approximation $U(q) = 2\pi e^2/\epsilon[q + (8\pi e^2/\epsilon)\rho_F]$ to give an indication of the importance of screening, although this approximation must fail for $E_F \to 0$ since it applies strictly only for disorder potential range much longer than the Fermi wavelength and $k_B T \ll E_F$. The density of states at the Dirac point ρ_F vanishes in the clean limit whereas it can be evaluated self consistently in the disordered case, leading to the small but finite value seen in the inset in Fig. 1(a). The inset in Fig. 1(c) compares the conductivity for unscreened and screened case at several different system sizes. We find that the conductivities evaluated with screened interactions are suppressed somewhat compared to the unscreened case. It appears likely that the precise value of $\sigma^{\min}$ may depend indirectly on electron-electron interactions.

We emphasize that we are able to evaluate the Kubo formula only over a relatively small range of finite system sizes. If we use the mobility to convert to physical length units the minimum system size we study is ~ 0.1 μm, not much smaller than the size of the crystallites studied experimentally [21]. Over the range of sizes we are able to study the conductivity does increase very slowly with system size, even at $E = 0$, as shown in the inset of Fig. 1(c). This weak size dependence might be hinting that the increasing conductivity predicted for two-dimensional systems with symplectic symmetry [28] by scaling arguments will emerge in the MDF model at extremely large system sizes even at $E = 0$. It is not obvious to us that the scaling theory applies at the Dirac point for either Coulomb or short-range scatterers since there is no length scale on which $\sigma \gg e^2/h$; the Fermi wavelength diverges as $E \to 0$, and then interference effects are hardly imagined. Alternately, the weak size dependence we find might be related to enhancement of carrier-density spatial fluctuations, which can be imagined in terms of puddles of electrons and holes, at larger system sizes in the long-range disorder potential case. Since Dirac fermions are not strongly localized, these puddles are not isolated but effectively percolate [29] and are constrained by boundary conditions in finite-size systems. The large length scale limit of the conductivity at zero temperature is more obvious for real graphene than for its MDF model, since intervalley scattering will always become relevant and lead to localization [14,16,17].

Finally, we comment on statistical properties of the conductivity and the resistivity at the Dirac point. Figure 1(d) shows the distribution function of the conductivity (main panel) and the resistivity (inset). The distribution function of σ has a sharp peak near $\sigma = (1/\pi)e^2/h$, and a large tail on the large σ regime. On the other hand,

the resistivity distribution function has a broad peak near h/e^2, as seen in experiment [21].

Discussion.—We find that a MDF model with Coulomb scatterers is able to account for two key findings of experiments on graphene sheets, namely, that the conductivity is proportional to the carrier density away from the Dirac point and that the minimal conductivity per channel is finite and larger than the SCBA value obtained theoretically for a MDF model with short-range scatterers. The impurity density n_i in the Coulomb model should be associated with the density of ionized impurities that are located in the substrate within a Fermi wavelength of the graphene plane. In this interpretation, the mobilities measured in current samples [21,22] correspond to $n_i \simeq 5 \times 10^{11}$ [cm^2]. The property that the conductivity is proportional to carrier density in the Boltzmann regime suggests dominant smooth intravalley scattering that could be Coulomb in character. If so, intervalley scattering is likely to be irrelevant in graphene in the Boltzmann transport regime, although it will always be important at finite carrier densities in the weak-localization regime when the temperature is low enough that the phase coherence length exceeds the intervalley scattering length, $l_0 \propto 1/|E_F|$. When intervalley scattering is weak, the MDF model applies and momentum-space Berry phases change constructive interference of back scattering particles into destructive interference [14,30], implying weak antilocalization. When local scatterers dominate in graphene intervalley and intravalley scattering rates [13,14,16] are comparable and the accumulated Berry phases are randomized, so that all states are localized [12,19]. In a weak magnetic field, the magnetic length limits the coherence of carriers. One recent magnetoresistance study has shown that highly doped graphene exhibits a negative magnetoresistance indicating weak localization, while states remain delocalized in the vicinity of the Dirac point [24]. These properties further support the view that graphene is described by a MDF model near the Dirac point. Our numerical results suggest that the MDF conductivity is finite and $\sim e^2/h$ at the Dirac point over the relevant range of the system size and the coherence length. In the presence of mesoscopic ripples in samples, the quantum corrections have been argued to be strongly suppressed. These issues come up with various interesting theoretical questions [24].

The authors acknowledge helpful interactions with A. Castro-Neto, V. Falko, A. Geim, E. Hwang, T. Hughes, Z. Jiang, J. Jung, P. Kim, and S. Ryu. This work has been supported by the Welch Foundation and by the Department of Energy under Grant No. DE-FG03-02ER45958.

Note added—After submitting the present Letter, we became aware of partly related work [31].

[1] J. C. Slonczewski and P. R. Weiss, Phys. Rev. **109**, 272 (1958).
[2] S. Deser, R. Jakiew, and S. Templeton, Phys. Rev. Lett. **48**, 975 (1982).
[3] G. W. Semenoff, Phys. Rev. Lett. **53**, 2449 (1984).
[4] E. Fradkin, E. Dagotto, and D. Boyanovsky, Phys. Rev. Lett. **57**, 2967 (1986).
[5] F. D. M. Haldane, Phys. Rev. Lett. **61**, 2015 (1988).
[6] E. Fradkin, Phys. Rev. B **33**, 3263 (1986).
[7] A. W. W. Ludwig, M. P. A. Fisher, R. Shankar, and G. Grinstein, Phys. Rev. B **50**, 7526 (1994).
[8] C. de C. Chamon *et al.*, Phys. Rev. Lett. **77**, 4194 (1996).
[9] D. H. Kim *et al.*, Phys. Rev. Lett. **79**, 2109 (1997).
[10] P. A. Lee, Phys. Rev. Lett. **71**, 1887 (1993).
[11] Y. Hatsugai and P. A. Lee, Phys. Rev. B **48**, 4204 (1993).
[12] Y. Morita and Y. Hatsugai, Phys. Rev. Lett. **79**, 3728 (1997); Phys. Rev. B **58**, 6680 (1998).
[13] N. H. Shon and T. Ando, J. Phys. Soc. Jpn. **67**, 2421 (1998).
[14] H. Suzuura and T. Ando, Phys. Rev. Lett. **89**, 266603 (2002).
[15] N. M. R. Peres, F. Guinea, and A. H. Castro Neto, Phys. Rev. B **73**, 125411 (2006).
[16] E. McCann *et al.*, Phys. Rev. Lett. **97**, 146805 (2006); D. V. Khveshchenko, Phys. Rev. Lett. **97**, 036802 (2006); A. F. Morpurgo and F. Guinea, Phys. Rev. Lett. **97**, 196804 (2006).
[17] M. I. Katsnelson, Eur. Phys. J. B **51**, 157 (2006); J. Tworzydlo *et al.*, Phys. Rev. Lett. **96**, 246802 (2006); K. Ziegler, Phys. Rev. Lett. **97**, 266802 (2006). I. L. Aleiner and K. B. Efetov, Phys. Rev. Lett. **97**, 236801 (2006); A. Altland, Phys. Rev. Lett. **97**, 236802 (2006).
[18] A. M. J. Schakel, Phys. Rev. D **43**, 1428 (1991); Y. Zheng and T. Ando, Phys. Rev. B **65**, 245420 (2002); V. P. Gusynin and S. G. Sharapov, Phys. Rev. Lett. **95**, 146801 (2005).
[19] D. N. Sheng *et al.*, Phys. Rev. B **73**, 233406 (2006).
[20] K. S. Novoselov *et al.*, Science **306**, 666 (2004).
[21] K. S. Novoselov *et al.*, Nature (London) **438**, 197 (2005).
[22] Y. B. Zhang *et al.*, Nature (London) **438**, 201 (2005).
[23] K. Nomura and A. H. MacDonald, Phys. Rev. Lett. **96**, 256602 (2006).
[24] S. V. Morozov *et al.*, Phys. Rev. Lett. **97**, 016801 (2006).
[25] D. J. Thouless and S. Kirkpatrick, J. Phys. C **14**, 235 (1981); Y. Imry, *Introduction to Mesoscopic Physics* (Oxford University, New York, 1997).
[26] P. A. Lee and T. V. Ramakrishnan, Rev. Mod. Phys. **57**, 287 (1985).
[27] T. Ando, J. Phys. Soc. Jpn. **52**, 1740 (1983); **53**, 3101 (1984); **53**, 3126 (1984).
[28] S. Hikami *et al.*, Prog. Theor. Phys. **63**, 707 (1980); Y. Asada *et al.*, Phys. Rev. B **73**, 041102 (2006); Physica (Amsterdam) **34E**, 228 (2006).
[29] M. I. Katsnelson, K. S. Novoselov, and A. K. Geim, Nature Phys. **2**, 620 (2006).
[30] T. Ando, T. Nakanishi, and R. Saito, J. Phys. Soc. Jpn. **67**, 2857 (1998).
[31] H. Kumazaki and D. Hirashima, J. Phys. Soc. Jpn. **75**, 053707 (2006); T. Ando, J. Phys. Soc. Jpn. **75**, 074716 (2006); E. H. Hwang and S. Das Sarma, cont-mat/0610561.